



**HAL**  
open science

## **In vitro and in vivo neurotoxicity of prion protein oligomers**

Steve Simoneau, Human Rezaei, Nicole Salès, Gunnar Kaiser-Schulz, Maxime Lefebvre-Roque, Catherine Vidal, Jean-Guy Fournier, Julien Comte, Franziska Wopfner, Jeanne Grosclaude, et al.

► **To cite this version:**

Steve Simoneau, Human Rezaei, Nicole Salès, Gunnar Kaiser-Schulz, Maxime Lefebvre-Roque, et al.. In vitro and in vivo neurotoxicity of prion protein oligomers. PLoS Pathogens, 2007, 3 (8), pp.1175-1186. 10.1371/journal.ppat.0030125 . hal-02666372

**HAL Id: hal-02666372**

**<https://hal.inrae.fr/hal-02666372>**

Submitted on 31 May 2020

**HAL** is a multi-disciplinary open access archive for the deposit and dissemination of scientific research documents, whether they are published or not. The documents may come from teaching and research institutions in France or abroad, or from public or private research centers.

L'archive ouverte pluridisciplinaire **HAL**, est destinée au dépôt et à la diffusion de documents scientifiques de niveau recherche, publiés ou non, émanant des établissements d'enseignement et de recherche français ou étrangers, des laboratoires publics ou privés.

# In Vitro and In Vivo Neurotoxicity of Prion Protein Oligomers

Steve Simoneau<sup>1</sup>, Human Rezaei<sup>2</sup>, Nicole Salès<sup>3</sup>, Gunnar Kaiser-Schulz<sup>4</sup>, Maxime Lefebvre-Roque<sup>1,3</sup>, Catherine Vidal<sup>5</sup>, Jean-Guy Fournier<sup>1</sup>, Julien Comte<sup>1</sup>, Franziska Wopfner<sup>4</sup>, Jeanne Grosclaude<sup>2</sup>, Hermann Schätzl<sup>4</sup>, Corinne Ida Lasmézas<sup>3\*</sup>

**1** Commissariat à l'Energie Atomique, Fontenay-aux-Roses, France, **2** Institut National de la Recherche Agronomique, Jouy-en-Josas, France, **3** Department of Infectology, The Scripps Research Institute, Jupiter, Florida, United States of America, **4** Institute of Virology, Technical University of Munich, Munich, Germany, **5** Institut Pasteur, Paris, France

**The mechanisms underlying prion-linked neurodegeneration remain to be elucidated, despite several recent advances in this field. Herein, we show that soluble, low molecular weight oligomers of the full-length prion protein (PrP), which possess characteristics of PrP to PrP<sup>Sc</sup> conversion intermediates such as partial protease resistance, are neurotoxic in vitro on primary cultures of neurons and in vivo after subcortical stereotaxic injection. Monomeric PrP was not toxic. Insoluble, fibrillar forms of PrP exhibited no toxicity in vitro and were less toxic than their oligomeric counterparts in vivo. The toxicity was independent of PrP expression in the neurons both in vitro and in vivo for the PrP oligomers and in vivo for the PrP fibrils. Rescue experiments with antibodies showed that the exposure of the hydrophobic stretch of PrP at the oligomeric surface was necessary for toxicity. This study identifies toxic PrP species in vivo. It shows that PrP-induced neurodegeneration shares common mechanisms with other brain amyloidoses like Alzheimer disease and opens new avenues for neuroprotective intervention strategies of prion diseases targeting PrP oligomers.**

Citation: Simoneau S, Rezaei H, Salès N, Kaiser-Schulz G, Lefebvre-Roque M, et al. (2007) In vitro and in vivo neurotoxicity of prion protein oligomers. *PLoS Pathog* 3(8): e125. doi:10.1371/journal.ppat.0030125

## Introduction

Transmissible spongiform encephalopathies are infectious neurodegenerative diseases. They are characterized by the accumulation in the brain, and sometimes the lymphoid tissues [1,2], of an abnormally structured form (PrP<sup>Sc</sup>) of the host prion protein (PrP) [3]. PrP<sup>Sc</sup> may constitute the infectious agent, also called prion, entirely [4] or in part [5,6]. The mechanism of neurodegeneration that ultimately leads to neuronal death and the occurrence of clinical symptoms, however, is still not known [7,8]. It has become apparent that immunohistochemically detectable PrP<sup>Sc</sup> aggregates, of various sizes ranging from fine granular deposition to amyloid plaques, do not represent the neurotoxic entity of prion diseases. Indeed, PrP<sup>Sc</sup> is not detectable in some cases of fatal familial insomnia [9], in lethal scrapie-like disease in mice overexpressing mutant PrP transgenes [10], in wild-type mice inoculated with bovine spongiform encephalopathy [11,12] or fatal familial insomnia [13], and in prion-infected mice with a P101L mutation in their PrP gene [14]. The hypothesis has been made earlier that the critical events in pathogenesis occur at the submicroscopic level [15].

On the other hand, PrP peptides comprising the hydrophobic domain (residues 106–126) of PrP are toxic to cultured neurons [16–19]. N-terminally truncated PrP also triggers neuronal death in the absence of expression of the normal form of the protein [20]. This shows that PrP has intrinsic properties that could render the protein toxic under certain conditions.

There is growing evidence that in other brain amyloidoses, prefibrillar soluble protein aggregates, rather than insoluble fibrils, are toxic [21–24]. In vivo, 56-kD dodecameric assemblies of A $\beta$ 1–42, dubbed A $\beta$ \* (of note, PrP\* has also been proposed as the biologically reactive form of PrP [25]), have been shown to be associated with memory deficits in a murine model of Alzheimer disease and to cause transient

memory impairment after injection in the brains of rats [26]. In a zebrafish model, expression of polyQ-expanded fragments of huntingtin lead to their accumulation as large SDS-insoluble cell inclusions; however, apoptotic cells are devoid of visible aggregates. Remarkably, the treatment with two anti-prion compounds prevented the formation of insoluble aggregates but did not suppress abnormal embryo morphology or cell death, strongly suggesting that upstream soluble huntingtin assemblies constitute the toxic culprit [27].

Recently, soluble oligomers presenting an enriched  $\beta$ -sheeted structure were proposed as intermediates in the amyloidogenesis process featured in prion diseases [28–31]. PrP oligomers were toxic in vitro [32,33].

We wanted to further investigate the hypothesis that prion diseases share a common mechanism of neurodegeneration with other brain amyloidosis, and set out to study the toxicity of PrP oligomers in vitro and in vivo in the presence or absence of endogenous PrP expression. We found that PrP oligomers exhibit considerably higher toxicity than PrP fibrils both in vitro and in vivo. PrP monomers were nontoxic. The toxicity occurred whether or not the neurons expressed PrP<sup>Sc</sup>. The toxicity of PrP oligomers could be abrogated by blocking the hydrophobic domain at the surface of the oligomers. We propose a comprehensive model of the possible mechanisms of prion-induced neurodegeneration.

**Editor:** Neil Mabbott, Roslin Institute, United Kingdom

**Received:** March 19, 2007; **Accepted:** July 10, 2007; **Published:** August 31, 2007

**Copyright:** © 2007 Simoneau et al. This is an open-access article distributed under the terms of the Creative Commons Attribution License, which permits unrestricted use, distribution, and reproduction in any medium, provided the original author and source are credited.

**Abbreviations:** LPrP, PrP ligand; PK, proteinase K; PrP, prion protein; PrP<sup>Sc</sup>, disease-associated form of PrP

\* To whom correspondence should be addressed. E-mail: lasmezas@scripps.edu

## Author Summary

Prion diseases are transmissible neurodegenerative diseases caused by an infectious agent thought to be composed mainly of a host protein, the prion protein (PrP). The mechanisms of neurodegeneration prevailing in these diseases are not well understood. In the present study, we demonstrate that small PrP aggregates, called oligomers, cause the death of neurons in culture and after injection in vivo. On the contrary, larger PrP aggregates, visualized as fibrils by electron microscopy, do not cause the death of cultured neurons and are much less toxic than PrP oligomers in vivo. We propose that the PrP oligomers exert their toxicity by disturbing neuronal membranes, as well as by an excessive intracellular concentration leading to the generation of death signals (also called apoptotic signals) by the cell. Moreover, the use of antibodies recognizing a certain portion of the PrP oligomers could prevent neuronal death. This study assigns prion diseases to the same group of diseases as Alzheimer disease, in which protein oligomers constitute the major trigger of the neurodegenerative process, and suggests new possible neuroprotective approaches for therapeutic strategies.

## Results

### Production and Characterization of PrP Oligomers

Two types of PrP oligomers were produced by either thermal refolding or expression of PrP in form of a tandem repeat.

A recombinant ovine PrP (23–234) was generated and converted into a  $\beta$ -sheeted form ( $\beta$ -PrP) (Figure 1A and 1B, left panel) by thermal refolding (see Materials and Methods and [34]). Both the  $\beta$ -sheeted and the  $\alpha$ -helical conformers had mobilities corresponding to a molecular weight of about 25 kDa by SDS-PAGE (Figure 1C, left panel).

Another type of PrP oligomer was created by exploiting the finding that dimerization has been described as a primary event in the PrP conversion and aggregation process [35]. Two monomeric PrP units were covalently linked head to tail via a flexible linker (Figure 1A, right panel). This protein displayed a molecular weight double that of the monomeric PrP in the presence of detergents (Figure 1C, right panel). The tandem murine PrP presents a higher  $\beta$ -sheeted content than the monomeric PrP as judged by the increase in the  $1,618\text{ cm}^{-1}$ -peak (Figure 1B, right panel). Size exclusion chromatography of both types of PrP preparations in physiological buffers showed that they were exclusively in an oligomeric state ([36] and Figure 1D). In summary, the tandem mouse PrP oligomerized spontaneously after purification, while the ovine PrP oligomerized after heating. These results are consistent with the recent finding that  $\alpha$ -PrP molecules convert into  $\beta$ -sheeted oligomers with a molten globule intermediate in the absence of any detectable  $\beta$ -sheeted monomeric PrP intermediate [37]. Both types of PrP oligomers showed slightly enhanced thioflavine T binding (Figure 1E), strongly suggesting that they were on the pathway of amyloid fibril formation (see below).

### Oligomeric PrP Is Slightly Proteinase K Resistant

We investigated whether oligomeric PrP was more resistant to proteinase K (PK) digestion than monomeric PrP. Each type of PrP was submitted to a range of PK concentrations. Both murine and ovine PrP oligomers exhibited partial resistance to PK digestion when compared to their respective monomeric counterparts (Figure 1C), as shown by i) the

difference in the degradation profile between the tandem PrP oligomers and the monomer at 500 ng/ml and 1  $\mu$ g/ml (the degradation of the tandem levels out, whereas the monomer continues to be degraded (compare arrows #1); ii) a PK-resistant core of the tandem of 36 kDa, which appears with increasing PK concentrations (see arrow #2); iii) the 20-kDa degradation product from the tandem increases with increasing concentrations of PK contrarily to the same 20-kDa product from the monomer (compare arrows #3); and iv) the residual  $\sim$ 25-kDa band of the ovine  $\beta$ -PrP observed at the PK concentration of 500 ng/ml (albeit weak, this signal was reproducible between experiments), contrasting with the complete digestion of ovine PrP monomers at the same concentration (arrows #4).

### Oligomeric PrP Is Neurotoxic to Mouse Cortical Neurons

We first analyzed the neurotoxic properties of the PrP oligomers in a murine primary cortical neuron model. Exposure of the neurons to both types of PrP oligomers resulted in a loss of nearly 50% of the neurons when compared to the untreated control cells, at a dose of 200  $\mu$ g/ml (Figure 2A) and 100  $\mu$ g/ml (Figure 2D), both corresponding to a concentration of 3  $\mu$ M. Hence, oligomeric PrP exhibited a roughly 30-fold higher toxic effect than the PrP peptide 105–132, which inserts into cellular membranes, and which induced 40% neuronal death at 100  $\mu$ M (Figure 2E). The same levels of toxicity were observed in PrP<sup>0/0</sup> neurons, indicating that the effect was not dependent on the expression of PrP by the cells (Figure 2B for murine PrP oligomers, data not shown for ovine PrP oligomers). We then wanted to verify that the seven-amino acid linker or the His expression tag present in the murine PrP oligomers were not responsible for their toxicity. Neither the linker, flanked on both sides by ten residues from the N- and C-terminal regions of the PrP sequence, (Figure 2C) nor grb-2 [38], an irrelevant protein of the same size as PrP (217 aa), generated in the same expression system as the tandem PrP and carrying the same His-tag, were toxic to the neurons (Figure 2A and data not shown).

To understand the type of neuronal death induced by these oligomers, the cells were analyzed morphologically using nuclear staining. Neuronal cultures treated with murine or ovine PrP oligomers (Figure 2F) revealed a high quantity of cells exhibiting condensed and fragmented chromatin, a hallmark of apoptosis.

### The Hydrophobic Domain of PrP Oligomers Is Essential for Toxicity

To identify the domains of PrP oligomers accountable for the observed toxicity, we occluded different regions of PrP oligomers by incubating them with a series of domain-specific PrP antibodies. Neurons exposed to murine or ovine PrP oligomers were fully protected against cell death using the monoclonal antibody Pri303 directed against the domain 106–126 of PrP (Figure 3 and data not shown). In contrast, incubation with the PrP monoclonal antibodies SAF84 (aa 161–170), Pri917 (aa 217–221), or SAF32 (aa 59–92) had no protective effect. These data show that the exposure of hydrophobic domain of PrP at the surface of the PrP oligomers is required for the neurotoxic mechanism. The effect of the various antibodies was similar on neurons expressing PrP or not (Figure 3), confirming in an independ-

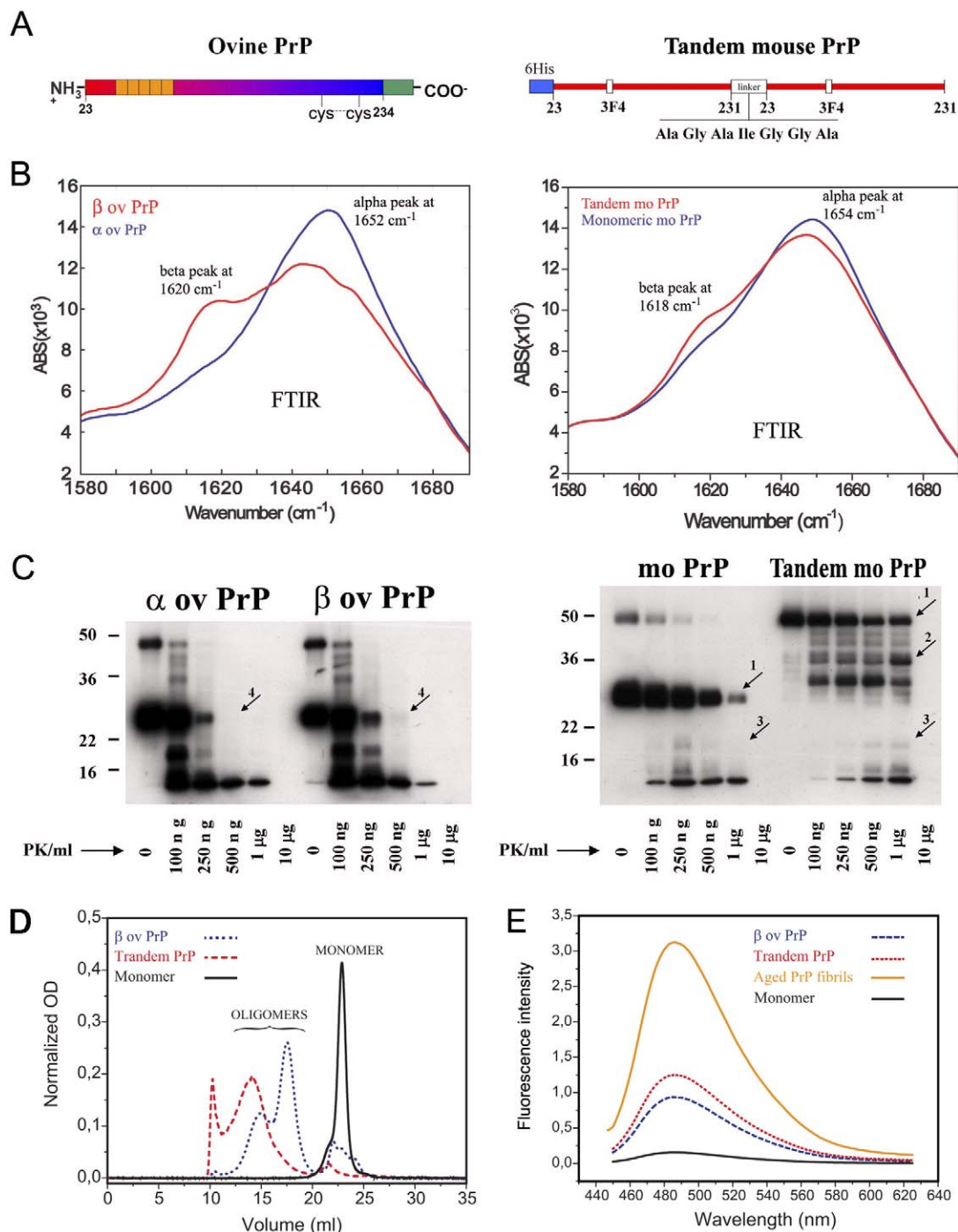


**Figure 1.** Characterization of PrP Species

(A) Molecular representation of the PrP proteins used. Left: ovine PrP. Right: covalently linked tandem PrP constructed by associating two mature murine PrP sequences (aa 23–231, not containing N- and C-terminal signal peptides) with a 7-amino acid linker sequence in a head-to-tail manner. The proteins were purified as described in the Materials and Methods section.

(B) Fourier transform infrared spectra (FTIR) of recombinant PrP proteins. Left: ovine  $\alpha$ -PrP (blue) and  $\beta$ -PrP (red). Right: monomeric (blue) and tandem (red) mouse PrP proteins. The results confirm the  $\beta$ -sheeted conformation of the  $\beta$ -PrP and indicate that the tandem PrP adopts a  $\beta$ -sheet-enriched conformation in physiological buffers.

(C) PK sensitivity of PrP species. PrP proteins were subjected to a PK digestion of 15 min at various concentrations of PK ranging from 100 ng/ml to 10  $\mu$ g/ml. Both ovine  $\beta$ -PrP (left) and mouse tandem PrP (right) exhibited partial protease resistance. The results are representative of at least two independent experiments. The numbered arrows point to locations where differences in PK resistance can be observed between monomeric and oligomeric PrP.

(D) Size exclusion chromatography performed on ovine PrP (black and blue lines) and covalently linked tandem PrP (red line) in PBS buffer, immediately after purification. The black line corresponds to the  $\alpha$ -helical ovine PrP monomers; the blue line corresponds to the refolded,  $\beta$ -sheeted ovine PrP preparations (very small monomeric peak, major bimodal oligomeric peak with an excess of 12 mers compared to the 36 mers); the red line corresponds to the murine tandem PrP preparations (very small monomeric peak, large oligomeric peak around the 36-mer peak of the ovine PrP oligomers, and sharp peak on the left corresponding to highly aggregated molecules that eluted in the amyloid void volume, V<sub>0</sub>).

(E) Thioflavine assay, which measures the fluorescence intensity of thioflavine bound to amyloiditic protein. Orange, fibrils of ovine PrP; blue, ovine PrP oligomers 15  $\mu$ M; red, murine tandem PrP oligomers 15  $\mu$ M; black, ovine monomers 15  $\mu$ M.

doi:10.1371/journal.ppat.0030125.g001

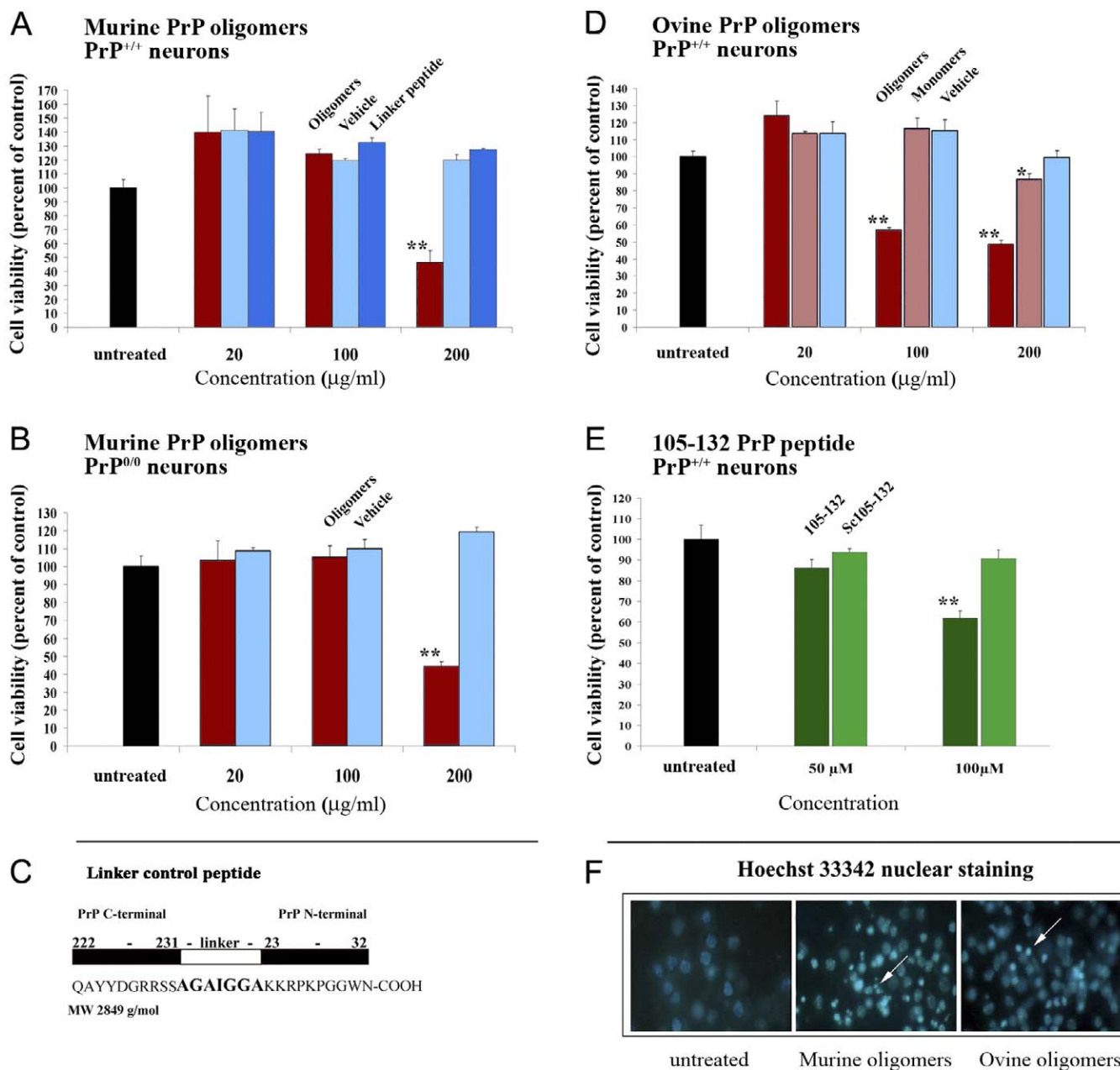


**Figure 2.** Neurotoxicity of Oligomeric PrP

(A–C) E15 cortical neurons from PrP<sup>+/+</sup> (A) or PrP<sup>0/0</sup> (B) were exposed to various concentrations of murine PrP oligomers (red bars) for 72 h, and then cell viability was measured using MTT. Untreated neurons (black bars) and neurons treated with either equivalent volumes of vehicle solution (light blue bars) or a peptide mimicking the linker region of the mouse tandem PrP (dark blue bars) were chosen as controls (see [C] for molecular details of the peptide).

(D) Cell viability measurements of neurons treated with either ovine PrP oligomers (dark red bars) or ovine PrP monomers (light red bars). The black and light blue bars correspond to untreated and treated with vehicle solution controls, respectively.

(E) To compare the toxicity of the PrP preparations with a known toxic PrP peptide, PrP<sup>+/+</sup> neurons were incubated with the PrP peptide 105–132 (dark green bars) and its scrambled version (light green bars) at two concentrations reported to induce neuronal death [18]. The cell viability results are expressed as a percentage relative to the untreated control (black bar) + SEM. The results are representative of at least two independent experiments performed with triplicate samples. The significance of the results was evaluated using a two-tailed unpaired student *t*-test with Welch corrections when needed (significant = \*, 0.01 < *p* ≤ 0.05; very significant = \*\*, *p* ≤ 0.01).

(F) Hoechst 33342 nuclear staining of embryonic cortical neurons incubated with toxic recombinant proteins. Left: No protein control, showing normal fully rounded cell nuclei. Middle: incubated with mouse PrP oligomers. Right: incubated with ovine PrP oligomers. Condensed nuclei characteristic of apoptotic cells are seen in treated cells (white arrows).

doi:10.1371/journal.ppat.0030125.g002

ent experiment that PrP oligomers are toxic to primary neurons regardless of the expression of PrP<sup>c</sup>, and showing that the prevailing neurotoxic mechanism can not be counteracted by endogenous PrP<sup>c</sup> present at the cell surface.

### PrP Fibrils Are Not Toxic on Primary Cortical Neurons

We then wanted to determine whether toxicity was limited to oligomeric PrP species or if PrP fibrils could also be toxic. We established that aging of PrP oligomers (a temperature-

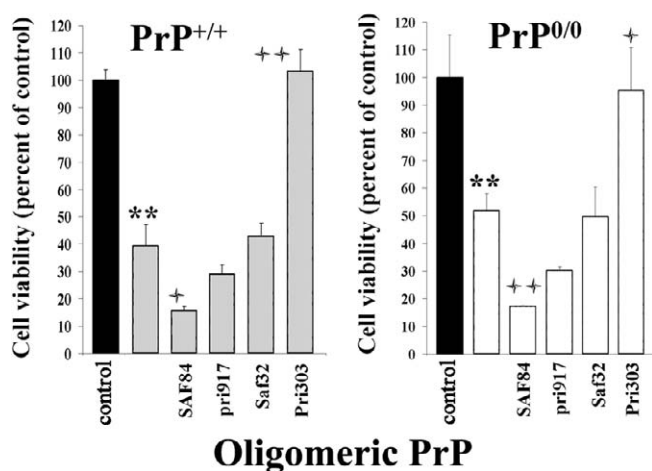


**Figure 3.** Rescuing of Oligomeric PrP-Induced Toxicity by Domain-Specific PrP Antibodies

Embryonic cortical neurons from PrP<sup>+/+</sup> (left, light gray bars) or PrP<sup>0/0</sup> (right, white bars) were incubated with 200 µg/ml (3 µM) of mouse PrP oligomers, in the presence or absence of PrP-specific monoclonal antibodies directed against different regions of the PrP protein (SAF32: 59–92; Pri303: 106–126; SAF84: 161–170; Pri917: 217–221). The results are expressed in terms of percentage relative to the untreated control (black bar). The graphs are representative of at least two independent experiments performed with triplicate samples. The significance of the results was evaluated using a two-tailed unpaired student *t*-test with Welch corrections when needed. \* indicates significance of values in relation to the untreated control (significant = \*, 0.01 < *p* ≤ 0.05; very significant = \*\*, *p* ≤ 0.01). + indicates significance of values in relation to the toxic dose (significant = +, 0.01 < *p* ≤ 0.05; very significant = ++, *p* ≤ 0.01).

doi:10.1371/journal.ppat.0030125.g003

dependent process, taking from minutes at 50 °C to one month at 4 °C) led to their polymerization into PrP fibrils. Figure 4A shows by electron microscopy that PrP oligomers exhibit a mixed granular and protofibrillar structure, while aged preparations form long mature fibrils 15 nm in diameter. These fibrils had amyloid properties as they strongly bound to thioflavine T (Figure 1E); they also showed enhanced PK resistance when compared to the PrP oligomers (not shown). Toxic PrP oligomers were soluble in sodium acetate, whereas aged PrP proteins were insoluble (Figure 4C, compare young and aged in the pellet fraction-P-). Fibrillar PrP preparations were not toxic, in contrast with oligomeric PrP (Figure 4B).

### PrP Oligomers Exhibit Higher Neurotoxicity than PrP Fibrils In Vivo, and the Toxicity Is Independent of Endogenous PrP Expression

To investigate the toxicity of different forms of PrP in vivo, stereotaxic subcortical injections of oligomeric or fibrillar PrP were carried out in the right hemispheres (ipsilateral) of C57BL/6 PrP<sup>+/+</sup> or C57BL/6 PrP<sup>0/0</sup> mice, and monomeric PrP or buffer alone was injected in the left hemispheres (contralateral). Table 1 and Figure 5 describe the experiments performed with ovine PrP preparations. The injection scheme is summarized in Table 1. Figure 5A shows the precise site of injection, just above the CA2 region of the hippocampus. The effect of the PrP preparations on neuronal toxicity was examined 24 h post-injection. The whole brains were sectioned and carefully screened for toxicity by

galloxyanine staining, even though toxicity was detected only at the expected site in the CA2 region of the hippocampus. No toxicity was observed in mouse brains injected with buffer alone or PrP monomers (Figure 5C, 5E, 5G, and 5I). PrP oligomers were highly toxic in both PrP-expressing and non-expressing mice, leading to an almost complete destruction of the pyramidal layer of neurons in the hippocampal region underneath the injection site (Figure 5D and 5H). Murine PrP oligomers were as toxic as ovine PrP oligomers (not shown). In vivo, PrP fibrils were also toxic but to a markedly milder extent than PrP oligomers (Figure 5B and 5F). To see if the neurons were dying by apoptosis, the cells were labeled with ApoptTag BrdU that binds to DNA breaks, a hallmark of apoptosis. As seen in Figure 6J and 6K, hippocampal neurons exposed to the toxic PrP oligomers exhibited intense BrdU labeling, which indicates that the neurons underwent apoptosis. Furthermore, the levels of BrdU labeling also provided a direct comparison of the level of toxicity of PrP oligomers versus PrP fibrils, showing again that the oligomers were more toxic than the fibrils.

In summary, these data show in vivo that soluble particles of PrP oligomers exert a high intrinsic neurotoxicity, whereas large PrP fibrils exhibit low neurotoxicity, both independently of endogenous PrPc expression.

### Discussion

There is a growing belief that intermediates in the formation of the protease-resistant prion protein PrP<sup>Sc</sup> (sometimes referred to as PrP\* [25]), rather than PrP<sup>Sc</sup> itself, are the pathogenic forms of PrP [10,11,13,14]. Moreover, there is evidence from other brain amyloidoses that soluble oligomeric forms of the disease-associated protein constitute the neurodegenerative trigger [21–24].

We tested this hypothesis using oligomeric β-sheeted PrP preparations. Throughout the study, we used two different types of PrP preparations in order to obviate a possible bias due to the method of oligomer preparation. One was a murine tandem PrP construct that spontaneously formed oligomers, while the other was an ovine PrP, the oligomerisation of which was induced by thermal refolding into β-sheeted PrP. Both have been characterized and used in previous studies [36,39]. We observed remarkably similar results with both types of oligomers in all the different experiments performed throughout this study. These oligomers were soluble in physiological buffers, showed mild PK resistance, and aggregated into insoluble amyloid fibrils upon aging, therefore resembling presumed PrP<sup>C</sup> to PrP<sup>Sc</sup> conversion intermediates. We first showed that β-PrP oligomers, but not α-PrP monomers, are toxic to cortical neurons in culture, in accordance with previous studies [32,33]. They were approximately 30 times more toxic than PrP peptides (Figure 2E and [18]). We did not observe a species-specific effect of murine versus ovine oligomers, suggesting that the main toxicity mechanism does not depend on a homologous interaction between PrP<sup>C</sup> and the PrP oligomers. In fact, the toxicity was completely independent of endogenous PrP expression by the neurons (Figure 2). The toxic effect of the β-PrP oligomers in PrP<sup>+/+</sup> and PrP<sup>0/0</sup> neurons could be reversed by blocking the 106–126 hydrophobic stretch of PrP with the Pri303 antibody, suggesting a direct role of this region in the toxicity. We have previously

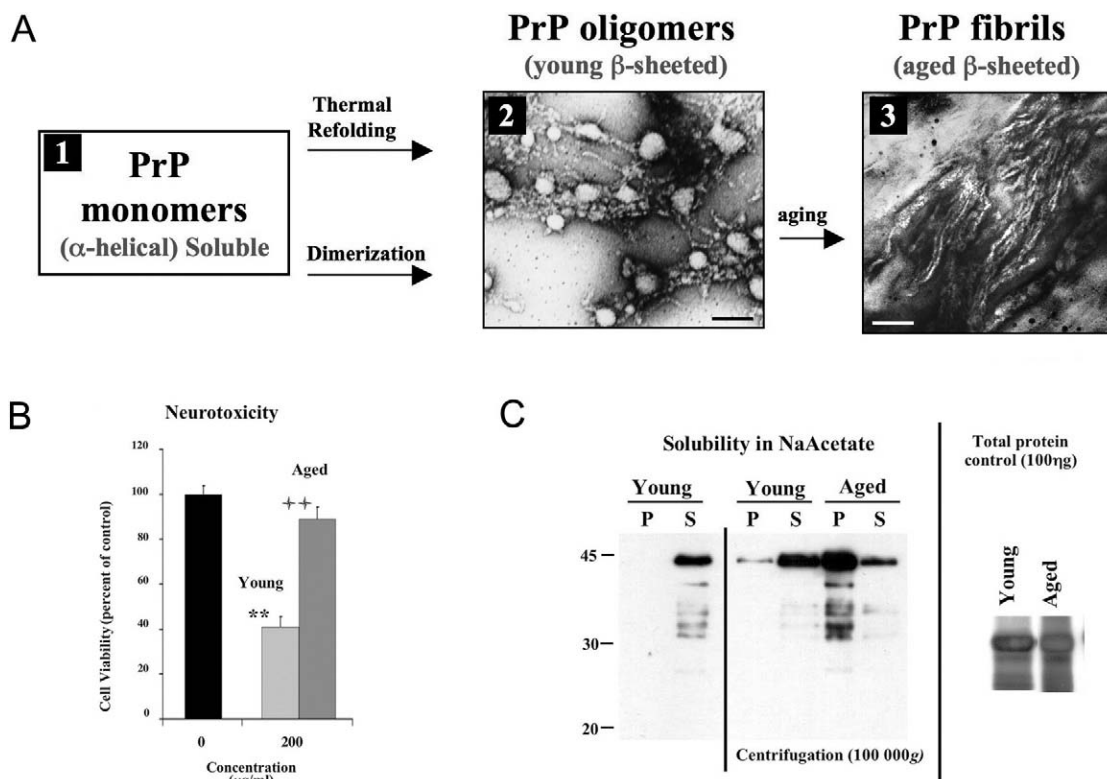


**Figure 4.** Relationship between PrP Ultrastructure, Solubility, and Neurotoxicity

(A) Electron microscopy analyses showing that PrP oligomers form granular aggregates and protofibrils (panel 2, scale bar = 100 nm). Upon aging, they assemble into long robust fibrils of PrP (panel 3, scale bar = 50 nm). Ovine PrP oligomers are shown in the pictures (panels 2 and 3), but similar results were obtained with murine tandem PrP oligomers.

(B) WST-1 cell viability measurements of cortical neurons treated with young (oligomeric) or aged (fibrillar) PrP showing that protofibrillar/oligomeric PrP is highly toxic, whereas fibrillar PrP is not toxic. The significance of the values was evaluated using a two-tailed unpaired student *t*-test with Welch corrections when needed. \* indicates significance of values in relation to the untreated control (very significant = \*\*,  $p \leq 0.01$ ). + indicates significance of values when compared with the toxic dose (very significant = ++,  $p \leq 0.01$ ).

(C) Solubility properties of PrP oligomers (young) and PrP fibrils (aged) in sodium acetate. Aged PrP forms insoluble aggregates as seen from the pellet fraction (P = pellet, S = supernatant). A total protein control shows that equal amounts of each protein were used (right panel). Murine PrP oligomers are shown in (B and C).

doi:10.1371/journal.ppat.0030125.g004

demonstrated the higher accessibility of hydrophobic clusters at the surface of our  $\beta$ -PrP oligomers by 1-anilino 8-naphthalene sulfonic acid (ANS) fluorescence probing [36]. It is a phenomenon common to protein misfolding [40], and

other authors have shown that the hydrophobic stretch 90–120 of PrP is available for antibody binding in  $\beta$ -oligomers [28]. Moreover, we have data (not shown) suggesting that  $\beta$ -PrP oligomers undergo an increased cellular uptake. One possible explanation is that the hydrophobic surface of the PrP oligomers favors their insertion into the lipid bilayer. This finding is in accordance with studies using PrP peptides encompassing the hydrophobic PrP domain, showing that they insert metastably into membranes and are toxic independently of PrPc expression [18,19]. Interestingly, the SAF84 antibody actually increased the toxicity of the PrP oligomers. This effect is not linked to its binding to cell surface PrPc, since it was observed in PrP-expressing and non-expressing cells. Because SAF84 binds to the S2-H2 hinge loop involved in the oligomerization process [41], a possible hypothesis is that it facilitates PrP oligomerisation and hence increases the toxicity.

Upon aging, toxic  $\beta$ -PrP oligomers assembled into insoluble fibrils that were not toxic on our primary cultures of cortical neurons. This finding is in accordance with the fact that the soluble, non-fibrillar amidated version of the hydrophobic PrP 106–126 peptide is toxic [42] and with the emerging view that the pathogenesis of amyloidotic diseases

**Table 1.** Experimental Set-Up of In Vivo Toxicity Assays

Mouse Number	Genotype	Left Hemisphere (Controls)	Right Hemisphere
1	PrP <sup>++</sup>	Buffer	PrP fibrils
2	PrP <sup>++</sup>	Monomeric PrP	PrP fibrils
3	PrP <sup>++</sup>	Monomeric PrP	PrP fibrils
4	PrP <sup>00</sup>	Buffer	PrP fibrils
5	PrP <sup>00</sup>	Monomeric PrP	PrP fibrils
6	PrP <sup>00</sup>	Monomeric PrP	PrP fibrils
7	PrP <sup>++</sup>	Buffer	Buffer
8	PrP <sup>00</sup>	Buffer	PrP oligomers
9	PrP <sup>00</sup>	Monomeric PrP	PrP oligomers
10	PrP <sup>00</sup>	Monomeric PrP	PrP oligomers
11	PrP <sup>++</sup>	Buffer	PrP oligomers
12	PrP <sup>++</sup>	Monomeric PrP	PrP oligomers
13	PrP <sup>++</sup>	Monomeric PrP	PrP oligomers

doi:10.1371/journal.ppat.0030125.t001

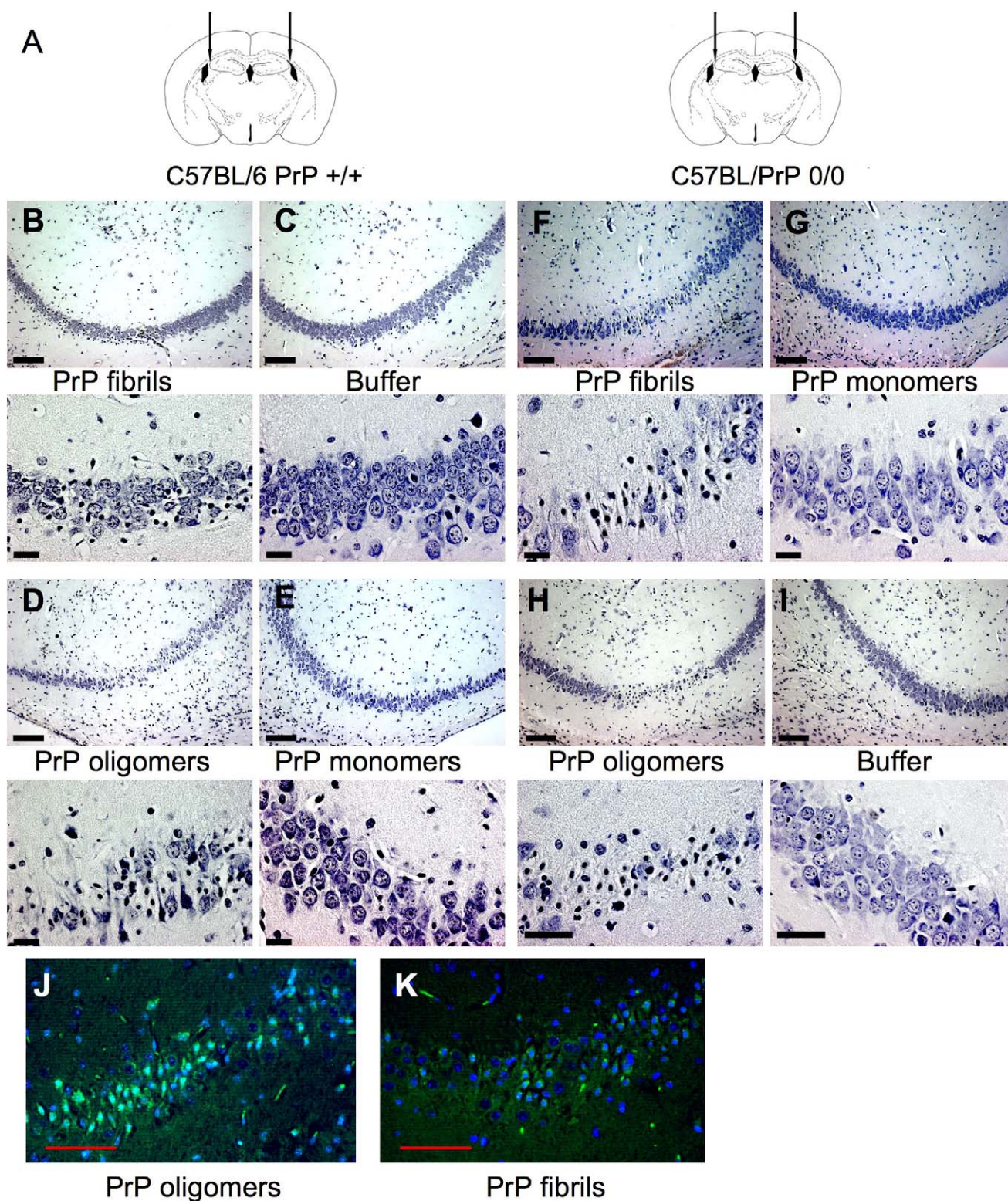


**Figure 5.** In Vivo Neurotoxicity of Ovine PrP Oligomers and Fibrils

(A) Schematic representation of a coronal section of a mouse brain with arrows indicating the injection sites of the PrP preparations. (B–I) Nissl-like staining (galloxyanine) of the hippocampal region CA<sub>2</sub>–CA<sub>3</sub> from the brains of mice injected with the PrP preparations or control buffer. Top panels represent the low magnification image (scale bar = 100 μm) and bottom panels the high magnification image (scale bar = 20 μm) of the lesioned regions (and anatomically corresponding region for the buffer and nontoxic PrP monomers). (B–E) Wild-type C57BL/6 mice, (F–I) PrP0/0 C57BL/6 mice.

(J and K) Higher toxicity of PrP oligomers versus PrP fibrils (wild-type C57BL/6 mice shown). Apoptotic pyramidal neurons in the lesioned hippocampal region have been labeled with the ApopTag BrdU kit and appear in green (scale bar = 50 μm).

doi:10.1371/journal.ppat.0030125.g005

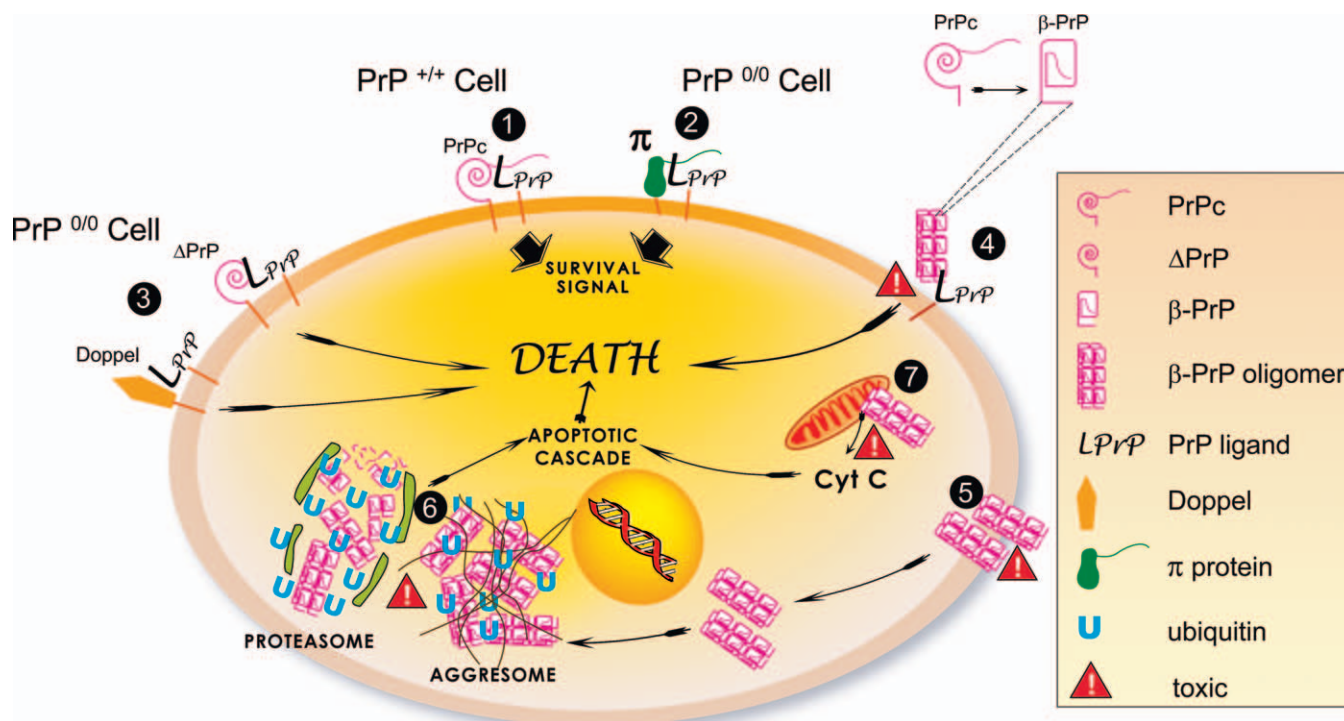


**Figure 6.** Model for the Mechanism of Oligomeric PrP-Induced Neurodegeneration

The scheme is derived from previous findings by other authors and has been complemented with mechanisms suggested by our data. (1) PrP interacts with its ligand LPrP on the cell surface to generate a signal necessary for cell survival. PrP binds to its natural ligand LPrP via its globular domain, while the interaction of the flexible N-terminus of PrP with LPrP triggers signal transduction [20,64]. (2) In a PrP knock-out cell,  $\pi$  can replace PrP for both binding and signal transduction [20,64]. (3) In experimental models where truncated forms of PrP ( $\Delta$ PrP) or Doppel (Dpl, a member of the PrP supergene family harboring partial sequence and structure similarity with PrP) are expressed on a PrP<sup>0/0</sup> background, binding of  $\Delta$ PrP or Dpl to LPrP occurs, but not signal transduction in the absence of a complete N-terminus [20,56,57,65]. Suppression of PrP or  $\pi$  signaling triggers cell death. (4) PrP oligomers present an altered interaction with LPrP. They bind, but do not trigger signal transduction, and thus by competition prevent PrPc (PrP<sup>+/+</sup> cells) or  $\pi$  (PrP<sup>0/0</sup> cells) binding to LPrP, resulting in cell lethality. (5) The hydrophobic domain of PrP at the surface of the oligomers enhances their insertion in the cellular membrane. This leads to membrane dysfunction, and hypothetically to the formation of pore-like structures [19,54] inducing toxic signals. (6) At high intracellular concentration, PrP oligomers accumulate in the aggresome [61] and saturate the proteasomal or other degradation pathways of the cell, leading to the generation of apoptotic signals. (7) The hydrophobic domain of PrP oligomers interact abnormally with mitochondrial membranes, leading to the release of cytochrome C (Cyt C) triggering the apoptotic cascade [66].  
doi:10.1371/journal.ppat.0030125.g006

is related to soluble oligomeric species rather than to high molecular weight protein assemblies [21,24]. We then wanted to verify *in vivo* the relevance of our *in vitro* findings. We performed stereotaxical injections of either the control solution, PrP monomers, PrP oligomers, or PrP fibrils in the supra-hippocampal region of C57BL/6 PrP<sup>+/+</sup> or C57BL/6 PrP<sup>0/0</sup> mice (Figure 5). First, we confirmed that  $\beta$ -PrP oligomers are highly toxic *in vivo*, both in PrP expressing or non-expressing mice. Like the *in vitro* experiments, the vehicle solution and  $\alpha$ -PrP monomers were not toxic to the neurons *in vivo*. As a comparison, 10  $\mu$ g of the 118–135 PrP peptide was toxic *in vivo* to retinal neurons after intravitreal inoculation [43]. Second, we found that PrP fibrils were toxic *in vivo*, but clearly less toxic than  $\beta$ -PrP oligomers. The same phenomenon was observed in PrP<sup>+/+</sup> and PrP<sup>0/0</sup> mice. This is clearly shown in Figure 5 by the differences in the extent of neuronal damage in the hippocampal cell layer and by the difference in BrdU labeling for apoptosis. The fact that PrP fibrils revealed some toxicity *in vivo* but not *in vitro* may be due to a different level of sensitivity of the neuronal subpopulation examined in either case (hippocampal versus cortical neurons), as well as an amplification of toxicity *in vivo* due to the presence of glial cells in the brain. Another

explanation may be that, *in vivo*, the fibrils were partially broken down into smaller, more toxic aggregates.

Another study showed *in vitro* that the toxicity of PrP oligomers and fibrils was dependent on the expression of PrP [33], suggesting the existence of alternative pathways of toxicity. Interestingly, the PrPc dependency of the PrP-induced toxicity has always been a matter of debate [17,44–46]. However, because these authors also observed a different toxicity behavior of their PrP fibrils *in vitro* than we did, we reason that all these differences may be due to the fibrils corresponding to different variants of supramolecular PrP assemblies. These variants would expose differently their reactive interface and thus react differently with the cell surface. Different shapes of PrP fibrils might be related with the “prion strain” phenomenon, causing the brain to degenerate more or less rapidly and triggering the death of different subset of neurons. Hence, apparent differences between our *in vitro* study and that by Novitskaya et al. teaches us that we may be revealing only different components of the very complex phenomenon of neurodegeneration induced by amyloidotic proteins. Therefore, while the dissection of mechanisms *in vitro* is obviously important, in

vivo approaches constitute the only way to assess their overall effect on the brain.

In vivo, endogenous PrP is required to generate PrP oligomers, but, as shown by our experiment where we have externally provided the toxic PrP species to PrP<sup>0/0</sup> cells, not to induce neuronal death. This is also in accordance with findings in a transgenic mouse model where prion replication and death of PrP<sup>0/0</sup> neurons occurred by exclusive astrocytic prion release [46]. In another study, conditional suppression of PrPc expression in neurons during murine prion infection led to a halt in the neurodegenerative process and behavioral alterations [47,48]. In this model however, even if PrPsc continued to accumulate, it was found restricted to astrocytes, and the absence of supply of toxic PrP species in the vicinity of neurons was probably key to the neuroprotective effect.

Our in vivo findings are in accordance with the emerging consensus that during prion diseases, small undetectable PrP aggregates, rather than plaque-type PrP deposits, are responsible for neuronal dysfunction and death. This is supported by the lack of correlation between neuronal death and the observation of PrP plaques in vivo [9,49,50]. Moreover, highly aggregated extracellular deposits of PrP in scrapie-infected “anchorless” transgenic mice exhibit very low toxicity, if any at all [51]. Even if not toxic, this amyloid PrP or another yet unknown component is infectious, as evidenced by transmission to wild-type mice. Interestingly, another recent study suggests dissociation also between the presence of Prp amyloid and prion infectivity [52]. In a previous study where focal PrPsc aggregates were found in PrP<sup>0/0</sup> mice grafted with PrP<sup>+/+</sup> tissue, no toxicity was observed, possibly due to the aggregation state of the PrPsc detected by immunohistochemistry [45].

The finding that soluble PrP oligomers, preceding the formation of PrP fibrils, are the main neurotoxic species in vivo, assigns prion diseases to the group of other brain amyloidoses, like Alzheimer and Parkinson disease, with regard to their mechanism of neurodegeneration [7]. The commonality of this mechanism is remarkable. It involves a conformational change of the protein monomer, leading to the formation of soluble aggregates, which become insoluble as the protofilaments grow into amyloid fibrils. An antibody recognizing common structural elements from different cytotoxic oligomers was able to inhibit their cellular toxicity, hinting at a commonality also in the primary targets of toxicity [22]. Because some amyloid proteins, like A $\beta$ , are located in the extracellular space, whereas others ( $\alpha$ -synuclein) are cytosolic, it is likely that cell membranes that are accessible from both compartments constitute one of these targets. The early prefibrillar aggregates of HypF-N (a disease-unrelated protein used as a model to study aggregate-forming, pathogenic proteins) were shown to be able to permeate synthetic phospholipid membranes [53]. Recently, the physical mechanism of toxicity associated with the intermediate-size A $\beta$  peptide oligomers was found to be the formation of conducting pores in lipid bilayers [54].

Figure 6 reviews the most probable scenarios of PrP-induced toxicity, showing how our data feed into the context of earlier findings. In this model, the toxicity of the PrP oligomers would be 3-fold: the first scenario is linked to the conformational change of oligomeric PrP, resulting in the loss of the N-terminal flexibility in the oligomers, which

thereby mimic the effect of  $\Delta$ PrP constructs described in earlier studies (Figure 6, #3 and #4); the second is the membrane insertion and destabilization of PrP oligomers, similar to the effects of PrP peptides (Figure 6, #5); and the third relates to the intracellular effects of PrP oligomers, comparable to those described with cytoplasmic PrP (mainly Figure 6, #6).

In normal cells, PrPc is thought to convey a survival message by interacting with a cell surface ligand, LPrP. Several studies have shown that the PrPc binding domain is located in the structured core of the protein while the activating domain is in the flexible N-terminus of the protein [20,55–57] (Figure 6, #1). One of the scenarios proposed is that in PrP<sup>0/0</sup> mice, a hypothetical functional homologue of PrP ( $\pi$ ) binds to LPrP and transduces the signal (Figure 6, #2). However, PrP<sup>0/0</sup> mice engineered to express an N-terminally truncated PrP, or a PrP truncated in the most C-terminal part of the flexible domain ( $\Delta$ PrP) or Doppel (a protein of the PrP supergene family that lacks the N-terminus equivalent of PrP), harbor a neurotoxic phenotype, because Doppel and  $\Delta$ PrP bind to LPrP with higher affinity than  $\pi$  but lack the domain responsible for the transduction of the survival message (this is the so-called Shmerling or Doppel effect; Figure 6, #3). In PrP oligomers, the N-terminus of PrP is thought to be buried [36] and hence the oligomers would behave similarly to Doppel or  $\Delta$ PrP with regard to their interaction with LPrP (Figure 6, #4). Cellular uptake of PrP oligomers is likely to induce intracellular toxicity by the accumulation of protein oligomers at the mitochondrial membrane, resulting in the release of cytochrome C and subsequent activation of the apoptotic cascade (Figure 6, #7), as suggested for Parkinson and Alzheimer diseases [58]. Finally, it has been shown that a highly concentrated intracellular abnormal PrP species is likely to end up accumulating in the aggresome/proteasome system [59,60]. Increased uptake and intracellular accumulation of PrP oligomers is likely to saturate intracellular degradation pathways like the proteasome, thereby triggering the apoptotic cascade (Figure 6, #6). The latter neurotoxic mechanism would also explain why most amyloid diseases are associated with old age, when there is likely to be an increased tendency of proteasome dysfunction and for proteins to become misfolded or damaged, in conjunction with the reduced efficiency of the molecular chaperone and unfolded protein responses [61,62].

The present study establishes  $\beta$ -PrP oligomers as a major neurotoxic species in vitro and in vivo, which likely represents the culprit PrP\* responsible for the development of transmissible spongiform encephalopathy-linked neurodegeneration. Targeting  $\beta$ -PrP oligomers, and their hydrophobic domain in particular, will allow researchers to devise rational neuroprotective treatments for these highly debilitating diseases.

## Materials and Methods

**Protein preparations.** The recombinant proteins used in this study were a monomeric mouse PrP sequence (23–231), a mouse tandem PrP composed of two monomeric sequences linked head to tail from the carboxy terminal to the amino terminal by a linker (flexible sequence) to allow for proper folding of the dimer, an  $\alpha$ -helical sheep PrP, and a  $\beta$ -sheeted version of the sheep PrP. The grb-2 protein and the linker sequence flanked at both sides by ten amino acids of the PrP sequence were used as control proteins.

Tandem PrP consists of two covalently linked murine PrP sequences without N- and C-terminal signal peptides. This recombinant protein was expressed and purified as previously described [41]. The proteins were stored at  $-20^{\circ}\text{C}$  in their elution buffer (8 M urea, 20 mM sodium phosphate, 500 mM sodium chloride, 500 mM imidazole, [pH 6.3]) until needed (see below).

The ovine PrP full-length protein was purified as described previously [64]. Briefly, the gene encoding the full-length ARQ variant (A136 R154 Q171) was cloned in pET 22b+ and expressed by IPTG induction in the *Escherichia coli* BL21 DE3 strain. After lysis, sonication, and solubilization of the inclusion bodies with urea, purification and renaturation of the prion protein were performed on an Ni Sepharose column by heterogeneous phase renaturation, taking advantage of the intrinsic affinity of the full-length protein for Ni.

For conversion, PrP (pH 7.2 in 20 mM MOPS) was heated at  $72^{\circ}\text{C}$  for 15 min and cooled to room temperature. Fourier transform infrared spectra confirmed that in these conditions, PrP forms oligomeric  $\beta$ -sheeted PrP. The characterization and mechanism of formation of these  $\beta$ -sheeted oligomers is published elsewhere [36]. Briefly, they form discrete 12-mer and 36-mer species, are oblate-shaped, have distinct secondary structure features, and display exposures of hydrophobic clusters.

The synthetic peptides used in this study were mouse PrP 105–132: KTNLKHVAGAAAAG-AVVGGLGGYMLGSA and mouse PrP scrambled 105–132: NGAGKAGMVGLYGAHG-ATAKVSLVGALA. They were prepared as described in [18].

**Storage and dialysis of proteins.** Mouse proteins were stored at  $-20^{\circ}\text{C}$  in their elution buffer (see above). The proteins were dialyzed just before use against ultrapure water or 10 mM sodium acetate (pH 4.5), and the concentration was obtained by the micro BCA protein assay. The sodium acetate did not affect the pH of the culture medium or the viability of the neurons at the dilutions used.

Sheep PrPs were produced just before use and kept at  $4^{\circ}\text{C}$  for a maximum of 30 d.

**Primary mouse cortical cultures.** PrP<sup>+/+</sup> mice used in this study were wild-type C57BL/6 mice. PrP<sup>0/0</sup> mice were obtained by backcrossing PrP knock-out mice, kindly provided by Charles Weissmann, with C57BL/6 mice over nine generations, and are therefore named C57BL/6 PrP<sup>0/0</sup> mice. Primary cortical cells were extracted from 15-d-old mouse embryos. Cortices were dissected under a binocular microscope in  $\text{Ca}^{2+}/\text{Mg}^{2+}$ -free PBS (Invitrogen, <http://www.invitrogen.com>) supplemented with glucose at a final concentration of 3%. Then, they were carefully freed of meninges and incubated in trypsin/EDTA solution (Eurobio, <http://www.eurobio.fr>) for 10 min at  $37^{\circ}\text{C}$ . The trypsin was removed and the leftover was inactivated with DMEM (Dulbecco's Modified Eagle's Medium, Invitrogen) containing 4.5 g/l glucose, Glutamax-I, and 1% FCS (fetal calf serum, Invitrogen). Cells were then mechanically dissociated using a flame-narrowed Pasteur pipette in the same culture medium. The cell suspension was then centrifuged and the pellet resuspended in DMEM supplemented with B27 (Invitrogen) and 3% FCS. Cells were seeded on plates coated with 10  $\mu\text{g}/\text{ml}$  of poly-D-lysine (Sigma, <http://www.sigmaaldrich.com>) initially in DMEM supplemented with B27 (2%), FCS (3%), and 100 U/ml penicillin/streptomycin. After 2 d, the culture medium was replaced by serum-free DMEM containing N2 supplements (1%; Invitrogen) and penicillin/streptomycin. Cultures were kept in a  $37^{\circ}\text{C}$  water-saturated incubator at 5%  $\text{CO}_2$ .

**In vivo neurotoxicity experiments.** Female C57BL/6 PrP<sup>+/+</sup> and C57BL/6 PrP<sup>0/0</sup> mice (see paragraph above) were anesthetized with isoflurane (1%–2.5%) and positioned on a stereotaxic frame. Once the bregma was identified and holes drilled, 2  $\mu\text{l}$  of 1 mg/ml of various PrP preparations or the same volume of buffer were injected into the hippocampus of the ipsi and contralateral hemispheres (1.5 mm posterior,  $\pm 2.00$  mm lateral, and 1.75 mm ventral to bregma, Figure 5A) at a rate of 0.4  $\mu\text{l}/\text{min}$ . The animals were killed by cervical dislocation at 24 h post-injection. The brains were dissected out, fixed in 4% buffered paraformaldehyde, and paraffin embedded. For the visualization of the neurons, 5- $\mu\text{m}$  horizontal sections from the mid-brain region were stained for nucleic acids with galocyanine according to standard protocols. To test for apoptosis, adjacent sections of selected brain sections were analyzed with the ApopTag BrdU kit according to the manufacturer's instructions (Molecular Probes, <http://probes.invitrogen.com>). Slides were examined on an epifluorescence Zeiss microscope (<http://www.zeiss.com>). All animal experiments were performed in accordance with national and European Union (EU) regulations.

**Proteinase sensitivity of PrP species.** Analysis of PK resistance was performed by incubating 10  $\mu\text{g}/\text{ml}$  of each protein for 15 min in the presence of various concentrations of PK at  $37^{\circ}\text{C}$ . The samples were

then precipitated with four volumes of methanol, resuspended in the loading buffer, and analyzed by western blot with the monoclonal antibodies 8G8 and Pri917 for the ovine and mouse PrP samples, respectively.

**In vitro neurotoxicity experiments.** For toxicity monitoring, cells were seeded at a density of  $7 \times 10^4$  cells per wells in a 96-well poly-D-lysine-coated plate (in each plate, only the 60 wells in the center contained cells and the outer wells were filled with PBS to prevent any drying). After 5 d in culture, neurons were incubated with the different recombinant PrP proteins for 72 h. In order to keep steady culture medium concentrations, the proteins were diluted in  $2\times$  culture medium and the proper volume of water and vehicle solution were added to get a final concentration of  $1\times$ . For controls, the cells were left untreated or were exposed to an equivalent volume of vehicle solution.

**Cell survival assays.** After exposure of the neurons to the proteins, the viability was measured either with MTT or with WST-1. For MTT, the medium was replaced with 500  $\mu\text{g}/\text{ml}$  of 3,[4,5 dimethylthiazol-2yl]-2,5 diphenyltetrazolium bromide (MTT; Sigma) dissolved in PBS. After 2 h of incubation at  $37^{\circ}\text{C}$ , the solution was removed and the blue formazan was solubilized with an isopropanol/HCL 1N (92:8) solution. Then, the optical density was measured at 540 nm with a reference wavelength of 630 nm. For WST-1 (Roche, <http://www.roche.com/>), 10  $\mu\text{l}$  of the reagent was added directly to the culture medium containing the cells and incubated for 1.5 h. Then, optical density measures were taken at 450 nm against a reference wavelength of 630 nm. In this case, a negative control, consisting of DMEM without cells, was used and subtracted from all samples.

**Visualization of apoptotic cells.** This was performed by staining cell nuclei with Hoechst 33342. Cells were seeded in poly-D-lysine-coated 8-well Labtek (Labtek II; Nalgen Nunc International, <http://www.nalgenunc.com/>) culture dishes at a density of  $1.6 \times 10^5$  cells/wells. After treatment with the recombinant proteins, the cells were mounted with Vectashield (Vector Laboratories, <http://www.vectorlabs.com/>) supplemented with 5  $\mu\text{g}/\text{ml}$  of Hoechst 33342 reagent (Molecular Probes). The slides were visualized using an axiovert (Zeiss) fluorescence microscope.

**Rescue experiments.** All monoclonal PrP antibodies used in this study have been purified with Protein-A or Protein-G affinity columns and dialyzed against ultra-pure water. These steps were carried out to remove growth factors and anti-microbial agents from the antibody solutions. Antibodies were added directly to the culture media containing the recombinant proteins of interest. Then these were incubated with the cells for 72 h.

**Electron microscopy of PrP samples.** All protein samples were first added (0.2–1.5 mg/ml) to serum-free DMEM containing N2 supplements (to be in the same conditions as the neurotoxicity experiments) and incubated for 2 h at  $37^{\circ}\text{C}$ . Following this step, a 10- $\mu\text{l}$  aliquot of protein preparation was applied to formvar- and carbon-coated grids. The excess fluid was drained with filter paper and the sample was stained for 1 min with 2% uranyl acetate. The grid was air-dried and examined in a Philips EM CM120 at 80 kV at a magnification of 15–75000.

**Solubility assay of PrP samples.** Young and aged PrP dimers were centrifuged at 100,000g for 1 h and the supernatant was separated from the pellet. The PrP was then visualized by western blot with the antibody 4H11.

**Thioflavine T fluorescence measurements.** Thioflavine T fluorescence measurements were performed at  $20^{\circ}\text{C}$  on a Jasco 6200 spectrofluorimeter (<http://www.jascoinc.co.jp/>) with a 1 mm  $\times$  10 mm optical path-length cuvette. The concentration of protein was adjusted to 15  $\mu\text{M}$  (equivalent monomer) for each species before incubation with 15  $\mu\text{M}$  thioflavine T. Excitation was performed at 432 nm.

## Acknowledgments

We thank Detlev Riesner for the analysis of the secondary structure of the covalent dimer and for helpful scientific discussions. We gratefully acknowledge Alun Williams for coordinating the EU project QLK3-CT-2001-00283 and Jan Langeveld, Christine Bauer, and Christian Spielhauer for provision of the PrP105–132 peptide, recombinant PrP, and grb-2 proteins. We thank Myriam Burel, Philippe Bozin, and Andrée Rouche for electron microscopy illustrations and assistance, as well as Alexandra Shermann for assistance in the histological analysis of the in vivo toxicity experiments. We thankfully acknowledge the insightful comments of Charles Weissmann. We are grateful to Amandine Roig for her artwork contribution (Figure 6).

**Author contributions.** SS and CIL conceived and designed the

experiments and wrote the paper. SS, HR, NS, GKS, MLR, CV, JGF, JC, and FW performed the experiments. SS, JG, HS, and CIL analyzed the data. HR and HS contributed reagents/materials/analysis tools.

## References

- Prusiner SB (1982) Novel proteinaceous infectious particles cause scrapie. *Science* 216: 136–144.
- Doi S, Ito M, Shinagawa M, Sato G, Isomura M, et al. (1988) Western blot detection of scrapie-associated fibril protein in tissues outside the central nervous system from preclinical scrapie-infected mice. *J Gen Virol* 69: 955–960.
- Pan KM, Baldwin M, Nguyen J, Gasset M, Serban A, et al. (1993) Conversion of  $\alpha$ -helices into  $\beta$ -sheets features in the formation of the scrapie prion proteins. *Proc Natl Acad Sci USA* 90: 10962–10966.
- Legname G, Baskakov IV, Nguyen HO, Riesner D, Cohen FE, et al. (2004) Synthetic mammalian prions. *Science* 305: 673–676.
- Couzin J (2004) Biomedicine. An end to the prion debate? Don't count on it. *Science* 305: 589.
- Weissmann C (1991) A 'unified theory' of prion propagation. *Nature* 352: 679–683.
- Caughey B, Lansbury PT (2003) Protofibrils, pores, fibrils, and neurodegeneration: Separating the responsible protein aggregates from the innocent bystanders. *Annu Rev Neurosci* 26: 267–298.
- Tagliavini F, Forloni G, D'Ursi P, Bugiani O, Salmons M (2001) Studies on peptide fragments of prion proteins. *Adv Protein Chem* 57: 171–201.
- Gambetti P, Parchi P, Petersen RB, Chen SG, Lugaresi E (1995) Fatal familial insomnia and familial Creutzfeldt-Jakob disease: Clinical, pathological and molecular features. *Brain Pathol* 5: 43–51.
- Telling GC, Haga T, Torchia M, Tremblay P, DeArmond SJ, et al. (1996) Interactions between wild-type and mutant prion proteins modulate neurodegeneration in transgenic mice. *Genes Dev* 10: 1736–1750.
- Lasmézas CI, Deslys JP, Robain O, Jaegly A, Beringue V, et al. (1997) Transmission of the BSE agent to mice in the absence of detectable abnormal prion protein. *Science* 275: 402–405.
- Manuelidis L, Fritch W, Xi YG (1997) Evolution of a strain of CJD that induces BSE-like plaques. *Science* 277: 94–98.
- Collinge J, Palmer MS, Sidle KCL, Gowland I, Medori R, et al. (1995) Transmission of fatal familial insomnia to laboratory animals. *Lancet* 346: 569–570.
- Manson J, Jamieson E, Baybutt H, Tuzi N, Barron R, et al. (1999) A single amino acid alteration (I01L) introduced into murine PrP dramatically alters incubation time of transmissible spongiform encephalopathy. *EMBO J* 18: 6855–6864.
- Flechsigs E, Shmerling D, Hegyi I, Raeber AJ, Fischer M, et al. (2000) Prion protein devoid of the octapeptide repeat region restores susceptibility to scrapie in PrP knockout mice. *Neuron* 27: 399–408.
- Forloni G, Angeretti N, Chiesa R, Monzani E, Salmons M, et al. (1993) Neurotoxicity of a prion protein fragment. *Nature* 362: 543–546.
- Brown DR, Schmidt B, Kretschmar HA (1996) Role of microglia and host prion protein in neurotoxicity of a prion protein fragment. *Nature* 380: 345–347.
- Haik S, Peyrin JM, Lins L, Rosseneu MY, Brasseur R, et al. (2000) Neurotoxicity of the putative transmembrane domain of the prion protein. *Neurobiol Dis* 7: 644–656.
- Bahadi R, Farrelly PV, Kenna BL, Kourie JI, Tagliavini F, et al. (2003) Channels formed with a mutant prion protein PrP(82–146) homologous to a 7-kDa fragment in diseased brain of GSS patients. *Am J Physiol Cell Physiol* 285: C862–C872.
- Shmerling D, Hegyi I, Fischer M, Blattler T, Brandner S, et al. (1998) Expression of amino-terminally truncated PrP in the mouse leading to ataxia and specific cerebellar lesions. *Cell* 93: 203–214.
- Stefani M, Dobson CM (2003) Protein aggregation and aggregate toxicity: New insights into protein folding, misfolding diseases and biological evolution. *J Mol Med* 81: 678–699.
- Kayed R, Head E, Thompson JL, McIntire TM, Milton SC, et al. (2003) Common structure of soluble amyloid oligomers implies common mechanism of pathogenesis. *Science* 300: 486–489.
- Taylor JP, Hardy J, Fischbeck KH (2002) Toxic proteins in neurodegenerative disease. *Science* 296: 1991–1995.
- Haass C, Selkoe DJ (2007) Soluble protein oligomers in neurodegeneration: Lessons from the Alzheimer's amyloid  $\beta$ -peptide. *Nat Rev Mol Cell Biol* 8: 101–112.
- Weissmann C, Enari M, Klohn PC, Rossi D, Flechsigs E (2002) Molecular biology of prions. *Acta Neurobiol Exp (Wars)* 62: 153–166.
- Lesne S, Koh MT, Kotilinek L, Kaye R, Glabe CG, et al. (2006) A specific amyloid- $\beta$  protein assembly in the brain impairs memory. *Nature* 440: 352–357.
- Schiffner NW, Broadley SA, Hirschberger T, Tavan P, Kretschmar HA, et al. (2007) Identification of anti-prion compounds as efficient inhibitors of polyglutamine protein aggregation in a zebrafish model. *J Biol Chem* 282: 9195–9203.
- Baskakov IV, Legname G, Baldwin MA, Prusiner SB, Cohen FE (2002) Pathway complexity of prion protein assembly into amyloid. *J Biol Chem* 277: 21140–21148.
- Baskakov IV, Legname G, Prusiner SB, Cohen FE (2001) Folding of prion protein to its native  $\alpha$ -helical conformation is under kinetic control. *J Biol Chem* 276: 19687–19690.
- Sokolowski F, Modler AJ, Masuch R, Zirwer D, Baier M, et al. (2003) Formation of critical oligomers is a key event during conformational transition of recombinant syrian hamster prion protein. *J Biol Chem* 278: 40481–40492.
- Govaerts C, Wille H, Prusiner SB, Cohen FE (2004) Evidence for assembly of prions with left-handed  $\beta$ -helices into trimers. *Proc Natl Acad Sci U S A* 101: 8342–8347.
- Kazlauskaitė J, Young A, Gardner CE, Macpherson JV, Venien-Bryan C, et al. (2005) An unusual soluble  $\beta$ -turn-rich conformation of prion is involved in fibril formation and toxic to neuronal cells. *Biochem Biophys Res Commun* 328: 292–305.
- Novitskaya V, Bocharova OV, Bronstein I, Baskakov IV (2006) Amyloid fibrils of mammalian prion protein are highly toxic to cultured cells and primary neurons. *J Biol Chem* 281: 13828–13836.
- Rezaei H, Choiset Y, Eghiaian F, Treguer E, Mentre P, et al. (2002) Amyloidogenic unfolding intermediates differentiate sheep prion protein variants. *J Mol Biol* 322: 799–814.
- Jansen K, Schafer O, Birkmann E, Post K, Serban H, et al. (2001) Structural intermediates in the putative pathway from the cellular prion protein to the pathogenic form. *Biol Chem* 382: 683–691.
- Rezaei H, Eghiaian F, Perez J, Doublet B, Choiset Y, et al. (2005) Sequential generation of two structurally distinct ovine prion protein soluble oligomers displaying different biochemical reactivities. *J Mol Biol* 347: 665–679.
- Gerber R, Tahiri-Alaoui A, Hore PJ, James W (2007) Oligomerization of the human prion protein proceeds via a molten globule intermediate. *J Biol Chem* 282: 6300–6307.
- Spielhaupt C, Schätzl HM (2001) PrPC directly interacts with proteins involved in signaling pathways. *J Biol Chem* 276: 44604–44612.
- Gilch S, Wopfner F, Renner-Muller I, Kremmer E, Bauer C, et al. (2003) Polyclonal anti-PrP auto-antibodies induced with dimeric PrP interfere efficiently with PrPSc propagation in prion-infected cells. *J Biol Chem* 278: 18524–18531.
- Dobson CM (2003) Protein folding and misfolding. *Nature* 426: 884–890.
- Eghiaian F, Daubenfeld T, Quenet Y, van Audenhaege M, Bouin AP, et al. (2007) Diversity in prion protein oligomerization pathways results from domain expansion as revealed by hydrogen/deuterium exchange and disulfide linkage. *Proc Natl Acad Sci U S A* 104: 7414–7419.
- Forloni G, Bugiani O, Tagliavini F, Salmons M (1996) Apoptosis-mediated neurotoxicity induced by  $\beta$ -amyloid and PrP fragments. *Mol Chem Neurobiol* 28: 163–171.
- Chabry J, Ratsimanoahatra C, Sponne I, Elena PP, Vincent JP, et al. (2003) In vivo and in vitro neurotoxicity of the human prion protein (PrP) fragment P118–135 independently of PrP expression. *J Neurosci* 23: 462–469.
- Fioriti L, Quaglio E, Massignan T, Colombo L, Stewart RS, et al. (2005) The neurotoxicity of prion protein (PrP) peptide 106–126 is independent of the expression level of PrP and is not mediated by abnormal PrP species. *Mol Cell Neurosci* 28: 165–176.
- Brandner S, Isenmann S, Raeber A, Fischer M, Sailer A, et al. (1996) Normal host prion protein necessary for scrapie-induced neurotoxicity. *Nature* 379: 339–343.
- Jeffrey M, Goodsir CM, Race RE, Chesebro B (2004) Scrapie-specific neuronal lesions are independent of neuronal PrP expression. *Ann Neurol* 55: 781–792.
- Mallucci G, Dickinson A, Linehan J, Klohn PC, Brandner S, et al. (2003) Depleting neuronal PrP in prion infection prevents disease and reverses spongiosis. *Science* 302: 871–874.
- Mallucci GR, White MD, Farmer M, Dickinson A, Khatun H, et al. (2007) Targeting cellular prion protein reverses early cognitive deficits and neurophysiological dysfunction in prion-infected mice. *Neuron* 53: 325–335.
- Bell JE, Ironside JW (1993) Neuropathology of spongiform encephalopathies in humans. *Br Med Bull* 49: 738–777.
- Gonzalez L, Martin S, Jeffrey M (2003) Distinct profiles of PrP(d) immunoreactivity in the brain of scrapie- and BSE-infected sheep: Implications for differential cell targeting and PrP processing. *J Gen Virol* 84: 1339–1350.
- Chesebro B, Trifilo M, Race R, Meade-White K, Teng C, et al. (2005) Anchorless prion protein results in infectious amyloid disease without clinical scrapie. *Science* 308: 1435–1439.
- Piccardo P, Manson JC, King D, Ghetti B, Barron RM (2007) Accumulation of prion protein in the brain that is not associated with transmissible disease. *Proc Natl Acad Sci* 104: 4712–4717.

53. Relini A, Torrasa S, Rolandi R, Gliozi A, Rosano C, et al. (2004) Monitoring the process of HypF fibrillization and liposome permeabilization by protofibrils. *J Mol Biol* 338: 943–957.
54. Singer SJ, Dewji NN (2006) Evidence that Perutz's double-beta-stranded subunit structure for beta-amyloids also applies to their channel-forming structures in membranes. *Proc Natl Acad Sci U S A* 103: 1546–1550.
55. Hundt C, Peyrin J-M, Haik S, Gauczynski S, Leucht C, et al. (2001) Identification of interaction domains of the prion protein with its 37-kDa/67-kDa laminin receptor. *EMBO J* 20: 5876–5886.
56. Baumann F, Tolnay M, Brabeck C, Pahnke J, Kloz U, et al. (2007) Lethal recessive myelin toxicity of prion protein lacking its central domain. *EMBO J* 26: 538–547.
57. Li A, Christensen HM, Stewart LR, Roth KA, Chiesa R, et al. (2007) Neonatal lethality in transgenic mice expressing prion protein with a deletion of residues 105–125. *EMBO J* 26: 548–558.
58. Hashimoto M, Rockenstein E, Crews L, Masliah E (2003) Role of protein aggregation in mitochondrial dysfunction and neurodegeneration in Alzheimer's and Parkinson's diseases. *Neuromolecular Med* 4: 21–36.
59. Ma J, Wollmann R, Lindquist S (2002) Neurotoxicity and neurodegeneration when PrP accumulates in the cytosol. *Science* 298: 1781–1785.
60. Kristiansen M, Messenger MJ, Klohn PC, Brandner S, Wadsworth JD, et al. (2005) Disease-related prion protein forms aggregates in neuronal cells leading to caspase activation and apoptosis. *J Biol Chem* 280: 38851–38861.
61. Nardai G, Csermely P, Soti C (2002) Chaperone function and chaperone overload in the aged. A preliminary analysis. *Exp Gerontol* 37: 1257–1262.
62. Csermely P (2001) Chaperone overload is a possible contributor to 'civilization diseases'. *Trends Genet* 17: 701–704.
63. Rezaei H, Marc D, Choiset Y, Takahashi M, Hui Bon Hoa G, et al. (2000) High yield purification and physico-chemical properties of full-length recombinant allelic variants of sheep prion protein linked to scrapie susceptibility. *Eur J Biochem* 267: 2833–2839.
64. Büeler H, Fischer M, Lang Y, Bluethmann H, Lipp H-P, et al. (1992) Normal development and behaviour of mice lacking the neuronal cell surface PrP protein. *Nature* 356: 577–582.
65. Moore RC, Mastrangelo P, Bouzamondo E, Heinrich C, Legname G, et al. (2001) Doppel-induced cerebellar degeneration in transgenic mice. *Proc Natl Acad Sci U S A* 98: 15288–15293.
66. O'Donovan CN, Tobin D, Cotter TG (2001) Prion protein fragment PrP-(106–126) induces apoptosis via mitochondrial disruption in human neuronal SH-SY5Y cells. *J Biol Chem* 276: 43516–43523.